Preliminary study for small animal preclinical hadrontherapy facility

G. Russo[a], P. Pisciotta[a,b,*], G.A.P. Cirrone[b], F. Romano[b], F. Cammarata[a], V. Marchese[a], G.I. Forte[a], D. Lamia[a], L. Minafra[a], V. Bravatá[a], R. Acquaviva[c], M.C. Gilardi[a], G. Cuttone[b]

[a] *Institute of Molecular Bioimaging and Physiology, IBFM CNR-LATO, Cefalú, Italy*
[b] *National Institute for Nuclear Physics, Laboratori Nazionali del Sud, INFN-LNS, Catania, Italy*
[c] *University of Catania, Catania, Italy*

ARTICLE INFO

Keywords:
Preclinical studies
Hadrontherapy
Geant4
Dosimetry
Small animal irradiation protocol

ABSTRACT

Aim of this work is the study of the preliminary steps to perform a particle treatment of cancer cells inoculated in small animals and to realize a preclinical hadrontherapy facility. A well-defined dosimetric protocol was developed to explicate the steps needed in order to perform a precise proton irradiation in small animals and achieve a highly conformal dose into the target. A precise homemade positioning and holding system for small animals was designed and developed at INFN-LNS in Catania (Italy), where an accurate Monte Carlo simulation was developed, using Geant4 code to simulate the treatment in order to choose the best animal position and perform accurately all the necessary dosimetric evaluations. The Geant4 application can also be used to realize dosimetric studies and its peculiarity consists in the possibility to introduce the real target composition in the simulation using the DICOM micro-CT image. This application was fully validated comparing the results with the experimental measurements. The latter ones were performed at the CATANA (Centro di AdroTerapia e Applicazioni Nucleari Avanzate) facility at INFN-LNS by irradiating both PMMA and water solid phantom. Dosimetric measurements were performed using previously calibrated EBT3 Gafchromic films as a detector and the results were compared with the Geant4 simulation ones. In particular, two different types of dosimetric studies were performed: the first one involved irradiation of a phantom made up of water solid slabs where a layer of EBT3 was alternated with two different slabs in a sandwich configuration, in order to validate the dosimetric distribution. The second one involved irradiation of a PMMA phantom made up of a half hemisphere and some PMMA slabs in order to simulate a subcutaneous tumour configuration, normally used in preclinical studies. In order to evaluate the accordance between experimental and simulation results, two different statistical tests were made: Kolmogorov test and gamma index test. This work represents the first step towards the realization of a preclinical hadrontherapy facility at INFN-LNS in Catania for the future *in vivo* studies.

1. Introduction

Molecular and cellular processes involved in hadrontherapy response are very complex and still not fully understood at all. Further studies are required for a full understanding of biological processes in hadrontherapy field. In fact, *in vitro* studies highlighted the complexity of mechanism which regulate cell response to ionizing radiations (apoptosis, necrosis, senescence, survival). Moreover, cell response was found to be strongly cell-type and dose dependent [1–3]. It was observed that radiations induce release of local and systemic inflammatory molecules and signal molecules, which communicate the damage to non-treated cells and tissues (bystander effects) [4,5]. Preclinical models represent the next step for the comprehension of biological processes and molecular mechanisms of response to radiation therapy, often used as a preliminary research for Phase 0 and Phase I human trials [6], with the aim of an application in clinical field [7]. The main purpose of this work is to lay down the foundation for the realization of a hadrontherapy preclinical facility in order to perform *in vivo* studies. Small animal irradiation systems must mimic the clinical application of radiation therapy as closely as possible. The irradiation technique has deeply evolved in the last years, producing new technologies such as the Intensity Modulated Radiation Therapy (IMRT) [8] that includes a highly conformal dose. The state of art is mainly focused on X-ray beam and, to achieve a preclinical treatment, different dose deposition systems were developed to allow dose deposition with high precision [9–12]. However, when tumours cannot be operated or are resistant to conventional radiation treatments, the hadrontherapy appears to be an efficient choice. Moreover, hadrontherapy is a necessary radiotherapy technique if tumour tissues are placed near to vital and sensitive organs, such as eyes, brain, colon,

* Corresponding author at: Institute of Molecular Bioimaging and Physiology, IBFM CNR-LATO, Cefalú, Italy.
E-mail address: pietro.pisciotta@ibfm.cnr.it (P. Pisciotta).

and so on. Hadrontherapy is able to deliver a high dose value to the tumour cells and limit the radiation absorption to healthy tissue and organs [13].

In order to perform preclinical research studies about the hadrontherapy effects on healthy tissues, it is essential to carry out the experimental measurements with a suitable experimental set-up. This set-up has to be dedicated to irradiations on small animals because the dose has to be delivered with high precision on the inoculated tumours. When ions are used, treatment planning for preclinical research application is far from being a routine, and a lot of work will be necessary before a complex dose distributions system could be used with high confidence.

An overview of specialized literature shows only a few works that include conformational proton irradiation of tumour in small animals [14–17]. An important aim of this work is to achieve a highly conformal dose to the target in small animal, avoiding irradiations of the surrounding healthy tissues and using clinical proton beam. Dose conformation covers an important role during radio-biological studies. In fact, the ionization radiation could induce on the healthy tissue, that surrounding the tumour area, DNA damage chromosomic aberration and secondary lesions. Proton-therapy reaches a good dose distribution on the target, mainly thanks to its characteristic depth-dose distribution due to the Bragg Peak. Another important issue during preclinical treatment is the dosimetry. In order to support more complex, individualized and conformal proton radiation experiments, it is necessary to develop an accurate Monte Carlo (MC)-based treatment planning system and use it as a valid support for the future *in vivo* studies. This MC approach can be helpful in order to design new medical treatment devices, to develope methods and optimize currently used treatment techniques. MC is, nowadays, the most powerful and precise computation tool for absorbed dose estimation and, in our specific case, it was essential to study and define all the requirements that a preclinical model involves. In this work, it was adopted the Geant4 toolkit [18,19], since it is able to simulate all the hadronic processes that occur from the interaction with the matter, and it has been validated several times comparing its results with experimental ones in a wide proton energy range. Using the previously mentioned simulation code, we developed an application that permits the simulation of all experimental set-up: experimental CATANA beam line and real target using its DICOM micro-CT images (Fig. 1).

Additional aim of our work is to perform a validation of our Geant4 application, comparing its results with experimental ones and realize a treatment simulation using a PMMA phantom that simulates a subcutaneous tumour in a mouse. Briefly, in this work a well-defined protocol to perform precise small animal irradiation and a home-made positioning and holding system in order to perform dosimetric measures using different solid phantom are developed.

2. Methods and materials

2.1. Experimental CATANA beam line

The experimental measurements were performed at the CATANA proton therapy facility, situated in Catania at INFN-LNS (Italy). It is, nowadays, used for radiotherapeutic treatment of eye tumours, such as choroidal or iris melanoma. When reaching the CATANA treatment room, proton beam of a maximum energy of 62 MeV/A goes out in the air and flies for 3 m before hitting the target. Through its path, the beam is intercepted by various elements and is modified in energy and shape in order to be used in clinical applications. Among these elements there are the scattering foils (to spread the beam laterally), collimators (to define beam profile in accordance to the tumour shape), monitor chambers (to measure the dose delivered) [20,21]. The presence of two x-ray tubes, positioned along and orthogonal to the beam direction, allows to verify the exact positioning of the target using radiopaque markers. Since the positioning system available in

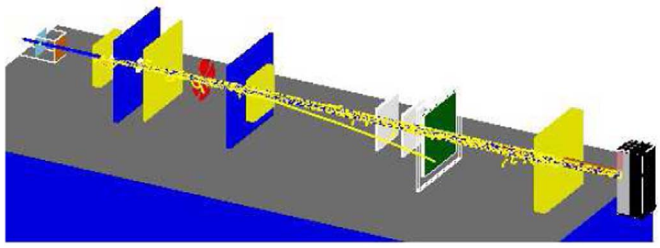

Fig. 1. CATANA beam line and phantom inserted in simulation framework using its DICOM CT images.

CATANA facility does not allow small animal irradiation, a holding system was designed and developed at INFN-LNS in order to perform precise and reproducible small animal irradiation with high precision level. This system can be integrated in the CATANA proton-therapy transport beamline to replace the positioning system used for patients.

2.2. Design and development of irradiation animal holder

This dedicated animal holder is basically a PMMA box designed and developed at INFN-LNS with a vertical pierced slab, on which a small animal can be fixed using bandages or cable ties. This vertical slab is fixed to the upper part of the box by means of a movable metallic cylinder that is able to move up and down, and around its axis, as indicated in Fig. 2 with white dashed line. In this way, it is possible to change the vertical position of the animal and the angle of incidence of the beam. Moreover, it is possible to move longitudinally the slab inside the box to provide sufficient space to put some PMMA thickness between the beam and the animal, in order to perform an energy degradation of the beam. In addition, a lateral door was added to make load/unload operations as easy as possible. Because of the possibility that anesthetized animals can urinate or lose some fur during irradiation time, the lower part of the box is without holes or slits, being designed as a sort of bowl.

2.3. Our geant4 application

The Geant4 application was developed using the Geant4 version 4.10.00 and it is based on these two different Geant4 examples: *hadrontherapy* [22–24] and DICOM [25]. Our application simulates the CATANA beam line geometry and the hadronic physic processes and it includes the capability to implement DICOM images as a target.

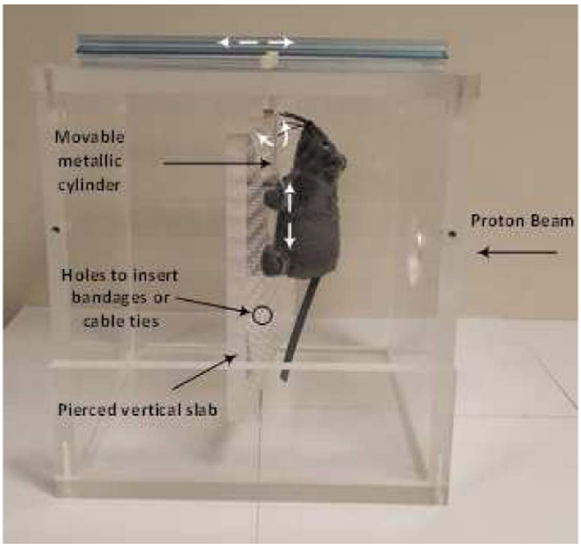

Fig. 2. Irradiation animal holder.

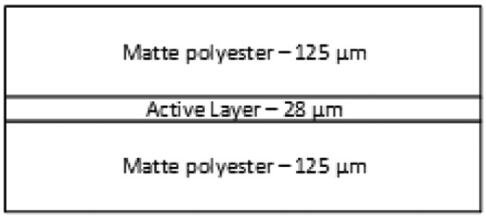

Fig. 3. Section of internal structure of EBT3 GafChromic film.

Using this application, we are able to reproduce and simulate the animal part that should undergo the irradiation and the areas around the tumour, such as bones, tissues, *etc.*. Anatomical structures can be inserted in the simulation set-up importing DICOM micro-CT images, transforming each voxel value of DICOM micro-CT images into a voxel of specific material inside the simulation environment. The assignment of material density is done following International Commission on Radiation Units and measurements (ICRU) report *n*0.46 [26]. In this way, it is possible to represent the materials that form the animal body (lung, liver, breast, bones, etc). Precision and attention to use appropriate CIRS phantom calibration is essential to perform accurate calibration of Hounsfield Unit (HU) of microCT scan. 3D dose maps can be evaluated for different beam configurations, such as the ones obtained using different modulator wheel, range shifter, collimator diameter, *etc.*, in order to choose the best animal treatment plan. The application permits to study more in detail the damage to the healthy tissue surrounding the tumour area to understand how properly the dose is delivered onto the targets inside the animal and estimate accurately the dose to the Organ at Risk (OAR). To treat the navigation in regular voxelised volumes, a special algorithm is used, called G4PhantomParameterisation/G4RegularNavigation. It is the fastest way without any extra memory requirement and it is the default in DICOM example. To properly calculate the dose in each voxel the G4PSDoseDeposit/RegNav scorer can be used [25]. Our application allows to reproduce the whole CATANA treatment beam line and implement DICOM micro-CT images as target in the simulation.

To validate our application, we compared simulation data with experimental ones obtained irradiating EBT3 Gafchromic film using CATANA proton beam.

2.4. EBT3-gafchromic film dosimetry

These films are a good choice for dosimetry measurements in clinical radiation oncology [27], due to their low energy dependence, high spatial resolution (around ten microns) and tissue-equivalence [28,29]. EBT3 Gafchromic^{TM} film model provided by Ashland was used for dosimetric measurements in PMMA phantom. It presents good characteristics to reproduce an ideal two-dimensional (2D) dosimeter thanks to its independence from energy and its high sensitivity [30]. Fig. 3 shows the dimension of each layer of the radiochromic film and Table 1 shows its atomic composition [31].

EBT3 film scans were performed by using a professional flatbed scanner Epson Expression 10000XL in transmission mode, producing 48 bit images with a resolution of 150 dpi, so providing a spatial resolution of 169 μm, and the resulting images were saved as no-compression TIFF file. During Gafchromic analysis only transmission data from red channel were used. Correct positioning (in order to obtain always the same position on scan plate) was ensured by a fixing system. The latter condition permits to use always the same central region of the scan plate, where response is uniform. Moreover, films were positioned for scanning using the same orientation as during the calibration and they were scanned 24 h after irradiation.

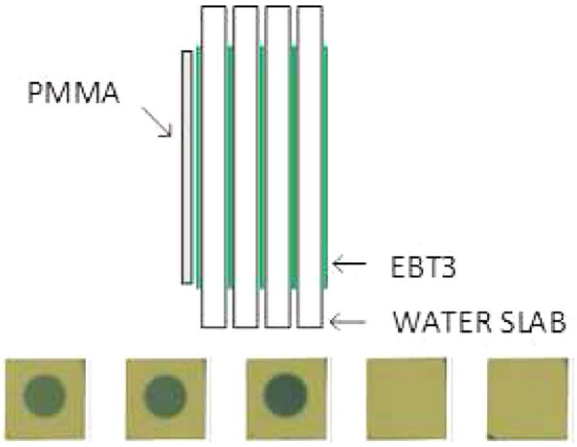

Fig. 4. Scheme of water solid phantom and irradiated EBT3 films.

2.5. The geant4 application validation

Validation of our application was performed comparing the 2D-dose distribution with the one obtained using the EBT3 gafchromic films inserted in a water solid (RW3) slab phantom, and the depth-dose profile with the one provided by a Markus Chamber. The water slabs were sandwich-like shaped, every layer of water slab being spaced out with a EBT3 layer. This phantom has been implemented in the simulation framework through its DICOM images obtained using a CT scan (GE Discovery STE-CT LightSpeed). The measurements consisted in irradiating a system made up of four squares, each 1 cm thick, of water phantom slabs with a layer of Gafchromic EBT3 put before and behind each slab, to form a kind of sandwich, as shown in Fig. 4. The five film pieces were cut into squares of $5 \times 5\ cm^2$ of dimension.

In particular, a 2.4 mm PMMA layer was placed in front of the stack, so that the first EBT3 film of the stack coincided with the calibration condition depth. Water slabs were irradiated with a pristine proton Bragg peak in order to release a dose of 3 Gy. In this way, it was possible to obtain information about the lateral dose distribution (along x- and y-axis) and the depth dose distribution (along beam axis), necessary to make a comparison with Geant4 simulation results.

2.6. The treatment simulation

A treatment simulation was performed to test the capability of the new Geant4 application to reproduce the dose distribution on small animals with a subcutaneous tumour, as normally used in preclinical studies. To simulate this situation, it was created a PMMA phantom: a half PMMA sphere that simulated a subcutaneous tumour in a mouse, and, as shown in Fig. 5. This is normally used in preclinical study to

Table 1
Dimensions of layers and nominal atomic abundances of GafChromic film EBT3.

Layer	Thickness	Density	Atomic percentage composition				
	[μm]	[g/cm^2]	C	H	O	Li	Al
Matte polyester	125	1.35	45.30	36.40	18.10	0.10	0.10
Active Layer	28	1.20	26.60	55.80	10.70	5.30	1.60

Fig. 5. Picture of PMMA phantom.

Fig. 6. 3D DICOM reconstruction of PMMA phantom.

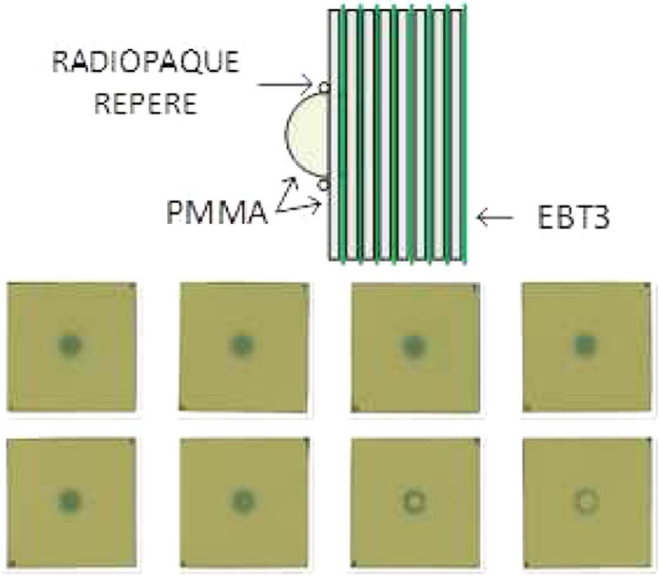

Fig. 7. Scheme of PMMA phantom and irradiated EBT3 films.

facilitate implantation/explantation operation and irradiation phases.

This phantom was implemented in our Geant4 application using its DICOM CT images, shown in Fig. 6. Subsequently, the simulated dose distribution was compared with experimental data provided by EBT3 Gafchromic films.

In this way, it was possible to verify if our Geant4 application could reproduce the experimental dose distribution obtained using EBT3 Gafchromic films, that were inserted in PMMA phantom, as shown in Fig. 7. This PMMA phantom, shown schematically in Fig. 7, was made up of one PMMA hemisphere of 8 mm diameter and of eight PMMA layers of $50 \times 50 \times 0.5$ mm^3. Between each layer a piece of 50×50 mm^2 EBT3 was inserted.

The good positioning of the target was verified using the two orthogonal X-ray tubes checking the markers on the images, as shown in Fig. 8. In this way it was possible to verify the correct position of the lesion in the mouse inside the animal holder.

The PMMA phantom was irradiated with a modulated proton beam to simulate a clinical treatment, with an 8 mm diameter collimator to shape the beam around the PMMA hemisphere. The Spread Out Bragg Peak (SOBP) was achieved using a modulator wheel together with a range shifter (21 mm equivalent in water). The resulting SOBP showed a practical range at 10% of 9.3 mm in water, a practical range at 90% of 8.5 mm in water, a SOBP width of 8.3 mm in water and a penumbra 90/10 of 0.8 mm in water. In this configuration, an 8 mm diameter collimator was used to shape the beam exactly around the hemisphere. The phantom was irradiated with a dose of 3 Gy (calibrated at center of the SOBP).

2.7. Data analysis

A test was performed to compare the 2D dose distribution obtained using Gafchromic films and the one obtained using the Monte Carlo simulations. For this purpose, it was developed a homemade Matlab script to implement the gamma index test. The gamma evaluation method is a combination between the dose difference and the DTA (Distance To Agreement) evaluation methods [32,33], which gives only binary results.

The gamma index is:

$$\gamma(\vec{r}_r) = min\{\Gamma(\vec{r}_e, \vec{r}_r)\} \ \forall \ \vec{\{}\, r_e\} \tag{1}$$

where

$$\Gamma(\vec{r}_e, \vec{r}_r) = \sqrt{\left(\frac{r^2(\vec{r}, \vec{r}_r)}{\Delta d^2}\right) + \left(\frac{\delta^2(\vec{r}, \vec{r}_r)}{\Delta D^2}\right)} \tag{2}$$

The expression $\vec{r}(\vec{r}_e, \vec{r}_r)$ is the spatial distance between the evaluated and the reference positions and $\delta(\vec{r}_e, \vec{r}_r) = D_e(\vec{r}_e) - D_r(\vec{r}_r)$, the dose difference between the two positions. The pass-fail criterion in this method will then indicate that when

$$\gamma(\vec{r}_r) \leq 1 \tag{3}$$

the calculation passes, whilst when

$$\gamma(\vec{r}_r) > 1 \tag{4}$$

the calculation fails. The gamma-index test was accomplished using the restriction of 3%/3 mm, commonly used in proton-therapy treatment plan and for highly conformal radiotherapy like IMRT [34].

3. Results

3.1. EBT3 calibration

The Gafchromic film calibration is mandatory before its use. This calibration was performed at CATANA proton beam line, using a Markus parallel-plate ionization chamber in a water phantom as reference, with twelve different Gafchromic pieces, that had been cut

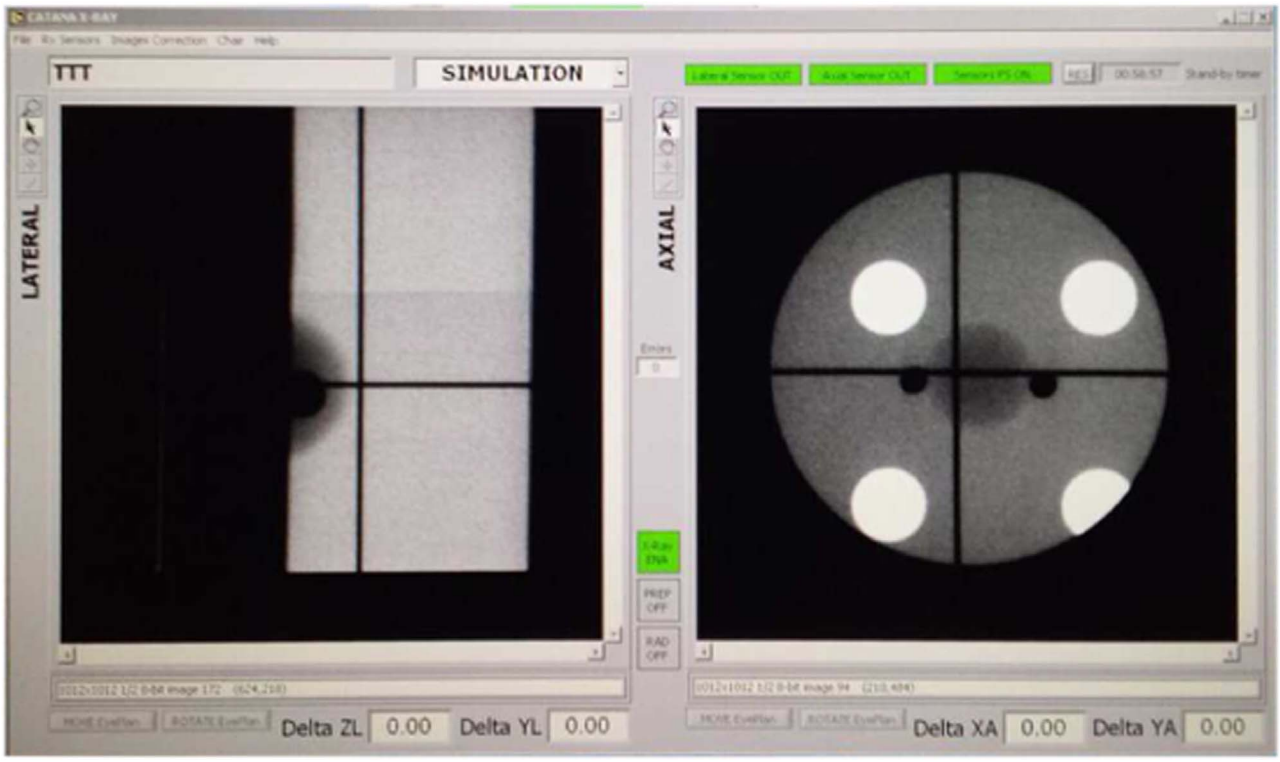

Fig. 8. Screenshot of CATANA software for X-ray tube management system.

in $3 \times 3\ cm^2$ squares. Only ten pieces of Gafchromic were irradiated with increasing doses (25 cGy, 50 cGy, 1 Gy, 2 Gy, 3 Gy, 5 Gy, 10 Gy, 15 Gy, 20 Gy, 25 Gy); the remaining were not irradiated and left as background reference. The irradiated films were positioned immediately behind 2.4 mm of PMMA, in order to reproduce the same condition of Markus chamber irradiation configuration. The beam is shaped so that Gafchromic film is positioned at the entrance of pristine Bragg peak, to reduce positioning errors.

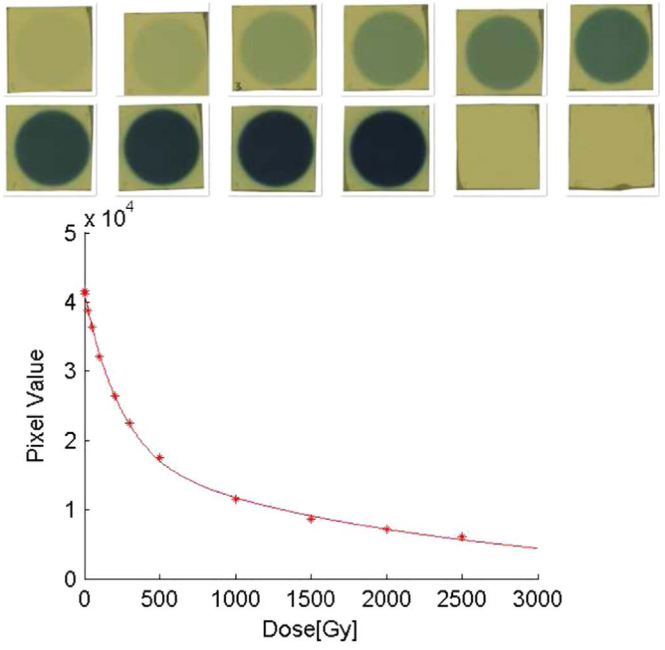

Fig. 9. Gafchromic films used for calibration and calibration curve. Red crosses represent gafchromic film measurements and blue line represents Gaussian best-fit. (For interpretation of the references to color in this figure legend, the reader is referred to the web version of this article.)

Fig. 9 shows the calibration curve obtained after Gafchromic analysis. In particular, the y-axis represents 16-bit pixel values (value between 0 and 65535), and the x-axis represents dose expressed in cGy. A gaussian algorithm called gauss2 in Matlab script is used to fit the curve.

3.2. Validation experimental results using water slabs

The Fig. 10 shows the comparison between the depth-dose distribution obtained with our customized Geant4 application (blue line) with the one measured using the Markus chamber (red crosses). A comparison between experimental horizontal and vertical profiles with the simulated ones, using the Geant4 toolkit, are shown in Fig. 11.

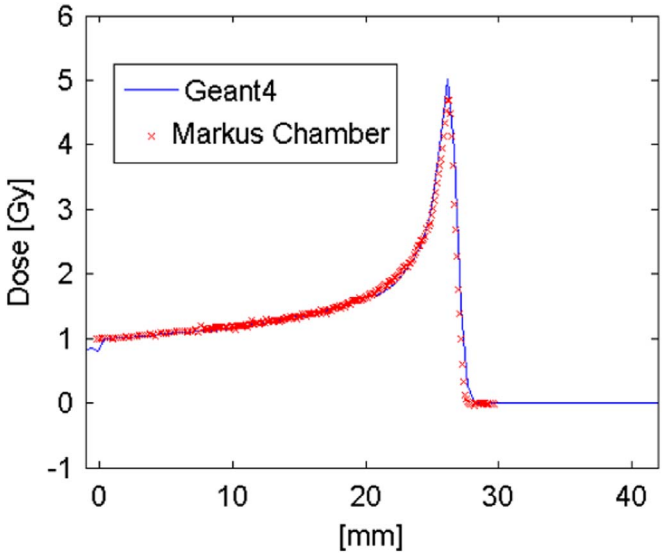

Fig. 10. Comparison between Geant4 and Markus chamber pristine Bragg peak profile using water phantom configuration.

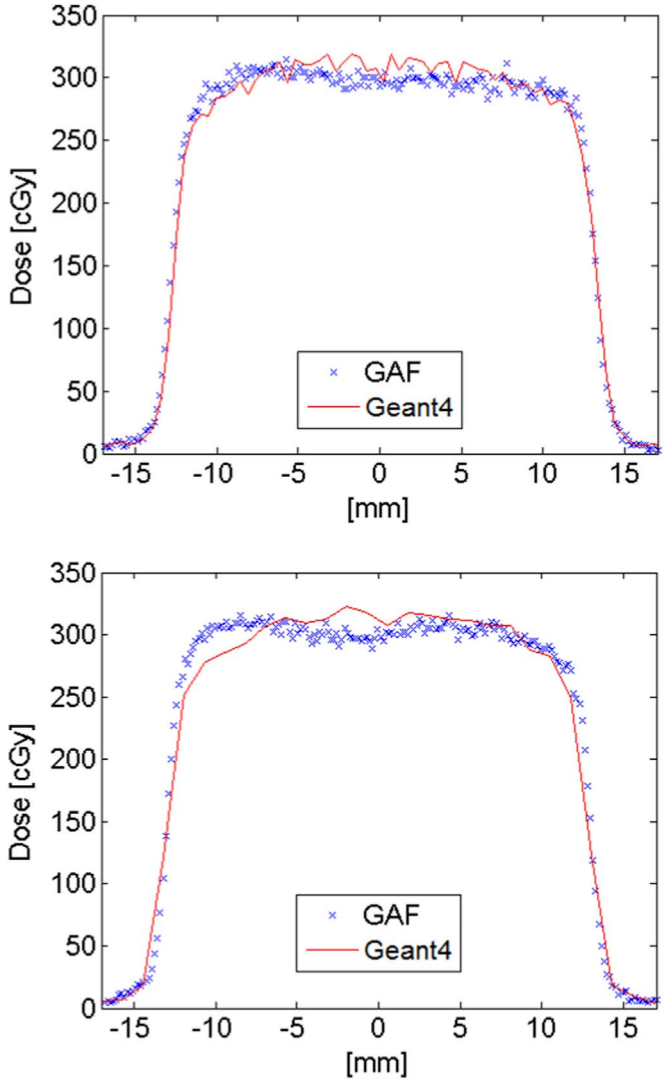

Fig. 11. Comparison between EBT3 and Geant4 beam profile along horizontal (up) and vertical (down) direction using water phantom configuration.

Table 2
Kolmogorov Test results for depth dose pristine Bragg peak in water phantom configuration.

Kolmogorov Test		
Pristine Bragg Peak	*P* value	*Test* result
Geant4 vs Markus Ch.	0.4215	*Passed*

Table 3
Kolmogorov Test results for horizontal and vertical profile in water phantom configuration.

Kolmogorov Test		
Pristine Bragg Peak	*P* value	*Test* result
X-profile: Geant4 vs EBT3	0.8883	*Passed*
Y-profile: Geant4 vs EBT3	0.8168	*Passed*

Experimental data fit quite well the simulated ones, except for a little asymmetry on the left upper side of the experimental vertical proton beam profile, that could be ascribed to a little vertical beam misalignment. Depth dose and transversal beam profile data appears in a quite good accordance as it is evident using the Kolmogorov-Smirnov test

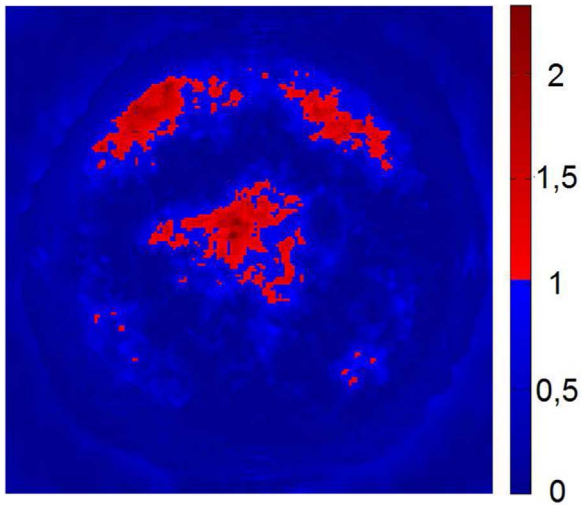

Fig. 12. Gamma index test results in water phantom configuration. Points that passed the test are shown in blue (from 0 to 1 on color scale) and points that failed the test are shown in red (more than 1 on color scale). (For interpretation of the references to color in this figure legend, the reader is referred to the web version of this article.)

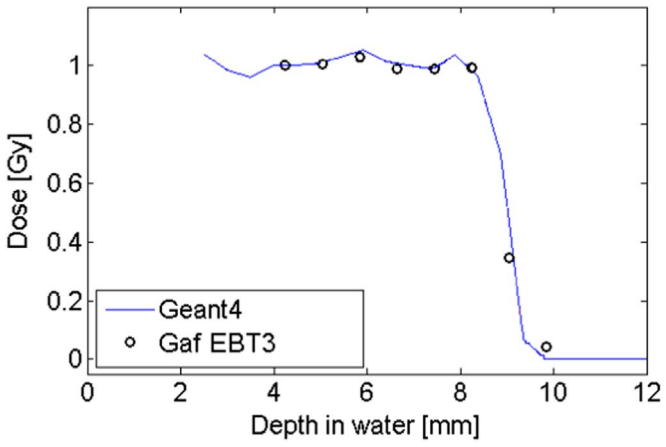

Fig. 13. Comparison between Geant4 (blue line) and EBT3 (black circle) SOBP depth dose profile using PMMA phantom configuration. (For interpretation of the references to color in this figure legend, the reader is referred to the web version of this article.)

[35]. Test results are shown in Tables 2, 3.

Gamma index test produces appreciable results when applied to our 2D dose distribution data. In particular, more than 94% of the points passed the test and only the residual percentage didn't, as shown in Fig. 12. This is due to an effective asymmetry of the beam, as noticed before during the profile analysis phase.

3.3. The treatment simulation results

Fig. 13 shows the comparison among the SOBP measured with the EBT3 stack and the one obtained through Geant4 simulation; black circles represent gafchromic measurements and blue line indicates simulation results.

Fig. 14 shows the comparison between beam profile along x- and y-axis measured with gafchromic films and calculated with Geant4 simulation.

In both previous cases, data accordance appears very good as it is evident from the Kolmogorov-Smirnov test results. Table 5 and Table 4 show the test results. The gamma index test was accomplished over a small area of the irradiated films, as shown in Fig. 15, to avoid in the analysis the reperi used to perform the alignment of the phantom. Test results appear again quite good and about 93% of the points passed the

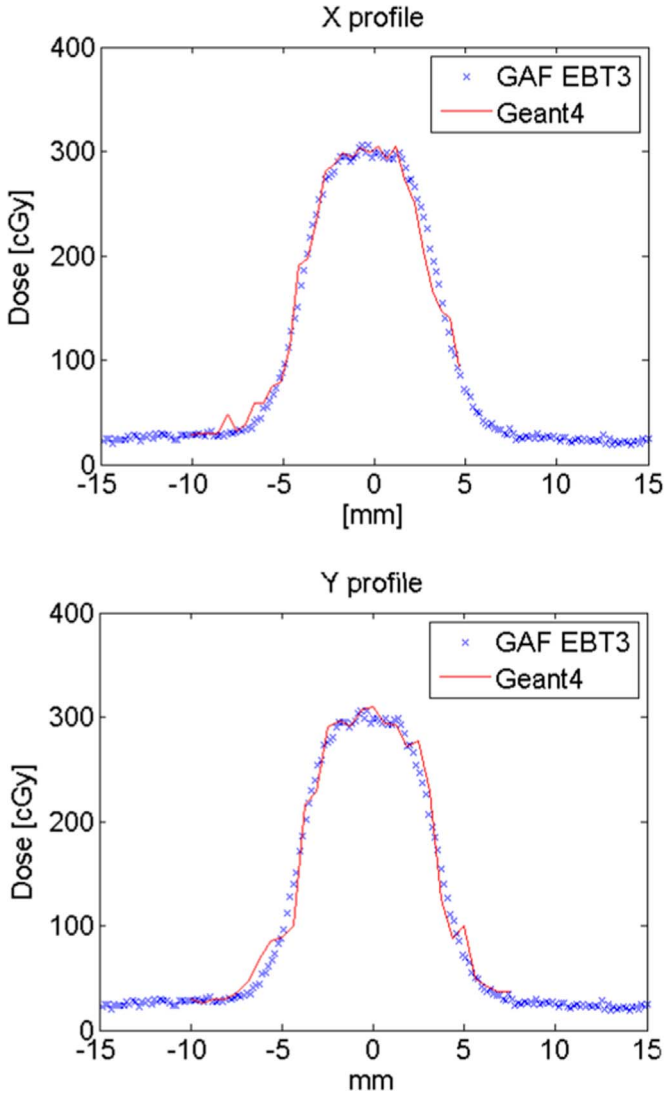

Fig. 14. Comparison between EBT3 and Geant4 profile along horizontal (up) and vertical (down) direction using PMMA phantom configuration.

Table 4
Kolmogorov Test results for SOBP in PMMA phantom configuration.

Kolmogorov Test		
SOBP	*P* value	*Test* result
Geant4 vs Markus Ch.	0.7016	*Passed*

Table 5
Kolmogorov Test results for horizontal and vertical profile in PMMA phantom configuration.

Kolmogorov Test		
SOBP	*P* value	*Test* result
X-profile: Geant4 vs EBT3	0.4263	*Passed*
Y-profile: Geant4 vs EBT3	0.3748	*Passed*

test, as shown in Fig. 16.

4. Discussion and conclusion

Preclinical studies represent an important step in the study of molecular mechanism induced inside the tumour cells in response to ionizing radiations. One of the aims of our work was to realize a system that permits to perform precise and consistent irradiation of tumour region in order to study molecular and biological processes involved during an hadrontherapy treatment. In this work, the ground to perform proton therapy preclinical studies was laid down. In fact, an irradiation platform was realized and tested to meet the requirements of mimicking the preclinical application of radiation therapy as closely as possible and of obtaining a highly conformal dose to the target, avoiding to irradiate the surrounding healthy tissues. This platform was used to perform both validation and treatment simulation at the CATANA proton therapy facility at INFN-LNS (Italy), using both unmodulated (pristine Bragg peak) and modulated (SOBP) proton beam with a maximum energy of 62 MeV/A. All the dosimetric measurements obtained were useful to determine the efficiency of our Geant4 application, to define the possibility to use it as a support to radiation treatment planning and, in particular, to define the best small animal irradiation condition. In fact, using our Geant4 application, it was possible to reproduce the real proton irradiation beam line and the real target geometry thanks to the opportunity of implementing small animal micro-CT images inside the simulation framework. The comparison between Geant4 simulation and experimental results using EBT3 Gafchromic Films and/or Markus chamber were resulted in good accordance. In detail, Kolmogorov tests were applied in order to study the accordance between the two datasets (experimental and simulated data) to compare the depth-dose curve and to compare the transversal profile (x- and y-profiles). Moreover, the gamma index test was applied for validating the simulated 2D dose distribution using the experimental ones obtained by EBT3 Gafchromic film. Gamma index test produced appreciable results when applied to our data. In particular, more than 94% of the points passed the test condition of 3%–3 mm using water slabs configuration and more than 93% of the points passed it (the test condition) using PMMA phantom configuration. Our Geant4 application proved to be a valid instrument to study the dose distribution in different type of phantoms with very variable geometry.

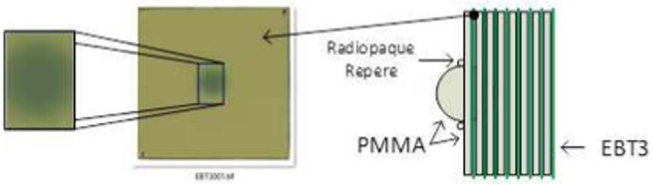

Fig. 15. Detail of the region used in the gamma index test in PMMA phantom configuration.

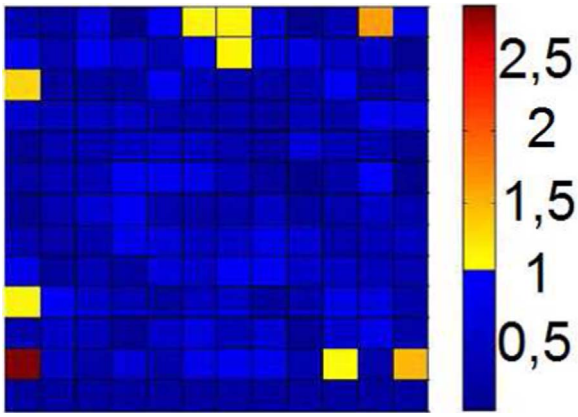

Fig. 16. Gamma index test result in PMMA phantom configuration. Points that passed the test are shown in blue (from 0 to 1 on color scale) and points that failed the test are shown in red (more than 1 on color scale). (For interpretation of the references to color in this figure legend, the reader is referred to the web version of this article.)

In the field of radiation oncology, the experimental design for mouse model may require specialized dosimetric techniques and innovative instruments to ensure that lethal or sub-lethal doses are delivered with sufficient accuracy. Additionally, it is necessary to be able to perform irradiation of a particular body part or system rather than the whole animal [36]. Our approach represents a good way to improve new radiation protocols respecting the laboratory animal science 3Rs, Replacement, Reduction and Refinement, to reduce the number of animals used, to improve the quality of science and to save time, money and other scientific resources [37]. In conclusion, this is a necessary preliminary work for the realization of a preclinical hadrontherapy facility at INFN-LNS and it lays down the foundation to implement interesting future *in vivo* studies using small animals.

Acknowledgements

The authors acknowledge the INFN Grant ETHICS for funding this work.

References

[1] M. Pucci, V. Bravatà, G.I. Forte, F.P. Cammarata, C. Messa, M.C. Gilardi, L. Minafra, Caveolin-1, breast cancer and ionizing radiation, Cancer Genom. Proteom. 12 (3) (2015) 143–152.

[2] L. Minafra, V. Bravatà, G. Russo, G.I. Forte, F.P. Cammarata, M. Ripamonti, G. Candiano, M. Cervello, A. Giallongo, G. Perconti, C. Messa, M.C. Gilardi, Gene expression profiling of MCF10A breast epithelial cells exposed to IOERT, Anticancer Res. 35 (6) (2015) 3223–3234.

[3] V. Bravatà, L. Minafra, G. Russo, G.I. Forte, F.P. Cammarata, M. Ripamonti, C. Casarino, G. Augello, F. Costantini, G. Barbieri, C. Messa, M.C. Gilardi, High-dose Ionizing Radiation Regulates Gene Expression Changes in the MCF7 Breast Cancer Cell Line, Anticancer Res. 35 (5) (2015) 2577–2591.

[4] F. Di Maggio, L. Minafra, G. Forte, F. Cammarata, D. Lio, C. Messa, M. Gilardi, V. Bravatà, Portrait of inflammatory response to ionizing radiation treatment, J. Inflamm. 12 (1) (2015) 14. http://dx.doi.org/10.1186/s12950-015-0058-3.

[5] L. Minafra, V. Bravatà, Cell and molecular response to IORT treatment (2014).

[6] J.G. Fox, S. Barthold, M. Davisson, C.E. Newcomer, F.W. Quimby, A. Smith, The Mouse in Biomedical Research: Diseases, 2nd, Academic Press, Amsterdam, Boston, 2007.

[7] M. Matinfar, E. Ford, I. Iordachita, J. Wong, P. Kazanzides, Image-guided small animal radiation research platform: calibration of treatment beam alignment, Phys. Med. Biol. 54 (4) (2009) 891–905. http://dx.doi.org/10.1088/0031-9155/54/4/005.

[8] E.B. Podgorsak, Radiation Oncology Physics : A Handbook for Teachers and Students, 2003.

[9] H. Deng, C.W. Kennedy, E. Armour, E. Tryggestad, E. Ford, T. McNutt, L. Jiang, J. Wong, The small-animal radiation research platform (SARRP): dosimetry of a focused lens system, Phys. Med. Biol. 52 (10) (2007) 2729–2740. http://dx.doi.org/10.1088/0031-9155/52/10/007.

[10] J. Wong, E. Armour, P. Kazanzides, I. Iordachita, E. Tryggestad, H. Deng, M. Matinfar, C. Kennedy, Z. Liu, T. Chan, O. Gray, F. Verhaegen, T. McNutt, E. Ford, T.L. DeWeese, High-resolution, small animal radiation research platform with x-ray tomographic guidance capabilities, Int. J. Radiat. Oncol. Biol. Phys. 71 (5) (2008) 1591–1599. http://dx.doi.org/10.1016/j.ijrobp.2008.04.025.

[11] M. Rodriguez, H. Zhou, P. Keall, E. Graves, Commissioning of a novel microCT/RT system for small animal conformal radiotherapy, Phys. Med. Biol. 54 (12) (2009) 3727–3740. http://dx.doi.org/10.1088/0031-9155/54/12/008.

[12] M. Bazalova, G. Nelson, J.M. Noll, E.E. Graves, Modality comparison for small animal radiotherapy: a simulation study, Med. Phys. 41 (1) (2014) 011710. http://dx.doi.org/10.1118/1.4842415.

[13] U. Linz (Ed.), Ion Beam Therapy, vol. 320 of Biological and Medical Physics, Biomedical Engineering, Springer Berlin Heidelberg, Berlin, Heidelberg, 2012. http://dx.doi.org/10.1007/978-3-642-21414-1

[14] C. Greubel, W. Assmann, C. Burgdorf, G. Dollinger, G. Du, V. Hable, A. Hapfelmeier, R. Hertenberger, P. Kneschaurek, D. Michalski, M. Molls, S. Reinhardt, B. Röper, S. Schell, T.E. Schmid, C. Siebenwirth, T. Wenzl, O. Zlobinskaya, J.J. Wilkens, Scanning irradiation device for mice in vivo with pulsed and continuous proton beams, Radiat. Environ. Biophys. 50 (3) (2011) 339–344. http://dx.doi.org/10.1007/s00411-011-0365-x.

[15] O. Zlobinskaya, C. Siebenwirth, C. Greubel, V. Hable, R. Hertenberger, N. Humble, S. Reinhardt, D. Michalski, B. Röper, G. Multhoff, G. Dollinger, J.J. Wilkens, T.E. Schmid, The effects of ultra-high dose rate proton irradiation on growth delay in the treatment of human tumor xenografts in nude mice, Radiat. Res. 181 (2) (2014) 177–183. http://dx.doi.org/10.1667/RR13464.1.

[16] N. Kondo, Y. Sakurai, T. Takata, N. Takai, Y. Nakagawa, H. Tanaka, T. Watanabe, K. Kume, T. Toho, S. Ichi Miyatake, M. Suzuki, S. Ichiro Masunaga, K. Ono, Localized radiation necrosis model in mouse brain using proton ion beams, Appl. Radiat. Isot. 106 (2015) 242–246. http://dx.doi.org/10.1016/j.apradiso.2015.07.032.

[17] T. Takata, N. Kondo, Y. Sakurai, H. Tanaka, T. Hasegawa, K. Kume, M. Suzuki, Localized dose delivering by ion beam irradiation for experimental trial of establishing brain necrosis model, Appl. Radiat. Isot. 105 (2015) 32–34. http://dx.doi.org/10.1016/j.apradiso.2015.07.023.

[18] S. Agostinelli, J. Allison, K. Amako, J. Apostolakis, H. Araujo, P. Arce, M. Asai, D. Axen, S. Banerjee, G. Barrand, F. Behner, L. Bellagamba, J. Boudreau, L. Broglia, A. Brunengo, H. Burkhardt, S. Chauvie, J. Chuma, R. Chytracek, G. Cooperman, G. Cosmo, P. Degtyarenko, A. Dell'Acqua, G. Depaola, D. Dietrich, R. Enami, A. Feliciello, C. Ferguson, H. Fesefeldt, G. Folger, F. Foppiano, A. Forti, S. Garelli, S. Giani, R. Giannitrapani, D. Gibin, J. Gómez Cadenas, I. González, G. Gracia Abril, G. Greeniaus, W. Greiner, V. Grichine, A. Grossheim, S. Guatelli, P. Gumplinger, R. Hamatsu, K. Hashimoto, H. Hasui, A. Heikkinen, A. Howard, V. Ivanchenko, A. Johnson, F. Jones, J. Kallenbach, N. Kanaya, M. Kawabata, Y. Kawabata, M. Kawaguti, S. Kelner, P. Kent, A. Kimura, T. Kodama, R. Kokoulin, M. Kossov, H. Kurashige, E. Lamanna, T. Lampén, V. Lara, V. Lefebure, F. Lei, M. Liendl, W. Lockman, F. Longo, S. Magni, M. Maire, E. Medernach, K. Minamimoto, P. Mora de Freitas, Y. Morita, K. Murakami, M. Nagamatu, R. Nartallo, P. Nieminen, T. Nishimura, K. Ohtsubo, M. Okamura, S. O'Neale, Y. Oohata, K. Paech, J. Perl, A. Pfeiffer, M. Pia, F. Ranjard, A. Rybin, S. Sadilov, E. Di Salvo, G. Santin, T. Sasaki, N. Savvas, Y. Sawada, S. Scherer, S. Sei, V. Sirotenko, D. Smith, N. Starkov, H. Stoecker, J. Sulkimo, M. Takahata, S. Tanaka, E. Tcherniaev, E. Safai Tehrani, M. Tropeano, P. Truscott, H. Uno, L. Urban, P. Urban, M. Verderi, A. Walkden, W. Wander, H. Weber, J. Wellisch, T. Wenaus, D. Williams, D. Wright, T. Yamada, H. Yoshida, D. Zschiesche, Geant4-a simulation toolkit, Nucl. Instrum. Methods Phys. Res. Sect. A Accel. Spectrometers , Detect. Assoc. Equip. 506 (3) (2003) 250–303. http://dx.doi.org/10.1016/S0168-9002(03)01368-8.

[19] J. Allison, K. Amako, J. Apostolakis, H. Araujo, P. Arce Dubois, M. Asai, G. Barrand, R. Capra, S. Chauvie, R. Chytracek, G. Cirrone, G. Cooperman, G. Cosmo, G. Cuttone, G. Daquino, M. Donszelmann, M. Dressel, G. Folger, F. Foppiano, J. Generowicz, V. Grichine, S. Guatelli, P. Gumplinger, A. Heikkinen, I. Hrivnacova, A. Howard, S. Incerti, V. Ivanchenko, T. Johnson, F. Jones, T. Koi, R. Kokoulin, M. Kossov, H. Kurashige, V. Lara, S. Larsson, F. Lei, O. Link, F. Longo, M. Maire, A. Mantero, B. Mascialino, I. McLaren, P. Mendez Lorenzo, K. Minamimoto, K. Murakami, P. Nieminen, L. Pandola, S. Parlati, L. Peralta, J. Perl, A. Pfeiffer, M. Pia, A. Ribon, P. Rodrigues, G. Russo, S. Sadilov, G. Santin, T. Sasaki, D. Smith, N. Starkov, S. Tanaka, E. Tcherniaev, B. Tome, A. Trindade, P. Truscott, L. Urban, M. Verderi, A. Walkden, J. Wellisch, D. Williams, D. Wright, H. Yoshida, Geant4 developments and applications, IEEE Trans. Nucl. Sci. 53 (1) (2006) 270–278. http://dx.doi.org/10.1109/TNS.2006.869826.

[20] N. Givehchi, F. Marchetto, L. Valastro, A. Ansarinejad, A. Attili, M. Garella, S. Giordanengo, V. Monaco, J.P. Montero, R. Sacchi, A. Boriano, F. Bourhaleb, R. Cirio, A. La Rosa, A. Pecka, C. Peroni, G. Cirrone, G. Cuttone, M. Donetti, S. Iliescu, S. Pittera, L. Raffaele, Online beam monitoring in the treatment of ocular pathologies at the INFN Laboratori Nazionali del Sud-Catania, Phys. Med. 27 (4) (2011) 233–240. http://dx.doi.org/10.1016/j.ejmp.2010.10.004.

[21] G. Cirrone, G. Cuttone, F. Di Rosa, S. Lo Nigro, M. Pia, L. Raffaele, G. Russo, Monte Carlo based implementation of an energy modulation system for proton therapy, in: Proceedings of the IEEE Symp. Conference Rec. Nucl. Sci. 2004, vol. 4, IEEE, 2004, pp. 2133–2137. http://dx.doi.org/10.1109/NSSMIC.2004.1462684

[22] G. Cirrone, G. Cuttone, Hadrontherapy: a Geant4-based tool for proton/ion-therapy studies, Prog. Nucl. Sci. 2 (2011) 207–212.

[23] G. Cirrone, G. Cuttone, F. Di Rosa, L. Raffaele, G. Russo, S. Guatelli, M. Pia, The GEANT4 toolkit capability in the hadron therapy field: simulation of a transport beam line, Nucl. Phys. B - Proc. Suppl. 150 (2006) 54–57. http://dx.doi.org/10.1016/j.nuclphysbps.2005.04.061.

[24] G. Cirrone, G. Cuttone, S. Guatelli, S. Lo Nigro, B. Mascialino, M. Pia, L. Raffaele, G. Russo, M. Sabini, Implementation of a new Monte Carlo-GEANT4 Simulation tool for the development of a proton therapy beam line and verification of the related dose distributions, IEEE Trans. Nucl. Sci. 52 (1) (2005) 262–265. http://dx.doi.org/10.1109/TNS.2004.843140.

[25] S. Chauvie, A. Armando, J. Madsen, DICOM - Readme (2014). URL ⟨http://geant4.web.cern.ch/⟩

[26] ICRU, Report No. 46, International Commission on Radiation Units and Measurements, 1968.

[27] J.F. Dempsey, D.a. Low, S. Mutic, J. Markman, A.S. Kirov, G.H. Nussbaum, J.F. Williamson, Validation of a precision radiochromic film dosimetry system for quantitative two-dimensional imaging of acute exposure dose distributions, Med. Phys. 27 (10) (2000) 2462–2475. http://dx.doi.org/10.1118/1.1290488.

[28] S.-T. Chiu-Tsao, T. Duckworth, C. Zhang, N.S. Patel, C.-Y. Hsiung, L. Wang, J.A. Shih, L.B. Harrison, Dose response characteristics of new models of GAFCHROMIC films: dependence on densitometer light source and radiation energy, Med. Phys. 31 (9) (2004) 2501. http://dx.doi.org/10.1118/1.1767103.

[29] L. Karsch, E. Beyreuther, T. Burris-Mog, S. Kraft, C. Richter, K. Zeil, J. Pawelke, Dose rate dependence for different dosimeters and detectors: tld, OSL, EBT films, and diamond detectors, Med. Phys. 39 (5) (2012) 2447–2455. http://dx.doi.org/10.1118/1.3700400.

[30] V. Casanova Borca, M. Pasquino, G. Russo, P. Grosso, D. Cante, P. Sciacero, G. Girelli, M.R.La. Porta, S. Tofani, dosimetric characterization and use of gafchromic ebt3 film for imrt dose verification, J. Appl. Clin. Med. Phys. 14 (2) (2013) 4111. http://dx.doi.org/10.1120/jacmp.v14i2.4111.

[31] G.A.P. Cirrone, G. Cuttone, G. Candiano, M. Carpinelli, E. Leonora, D.L. Presti, A. Musumarra, P. Pisciotta, L. Raffaele, N. Randazzo, F. Romano, F. Schillaci, V. Scuderi, A. Tramontana, R. Cirio, F. Marchetto, R. Sacchi, S. Giordanengo, V. Monaco, Absolute and relative dosimetry for ELIMED, in: 2ND ELIMED Work. PANEL, vol. 1546, AIP Publishing, 2013, pp. 70–80. http://dx.doi.org/10.1063/1.

4816609
[32] D.A. Low, W.B. Harms, S. Mutic, J.A. Purdy, A technique for the quantitative evaluation of dose distributions, Med. Phys. 25 (5) (1998) 656. http://dx.doi.org/10.1118/1.598248.
[33] W.B. Harms, D.A. Low, J.W. Wong, J.A. Purdy, A software tool for the quantitative evaluation of 3D dose calculation algorithms, Med. Phys. 25 (10) (1998) 1830. http://dx.doi.org/10.1118/1.598363.
[34] D.A. Low, J.F. Dempsey, Evaluation of the gamma dose distribution comparison method, Med. Phys. 30 (9) (2003) 2455. http://dx.doi.org/10.1118/1.1598711.
[35] F.J. Massey, The Kolmogorov-Smirnov Test for Goodness of Fit, J. Am. Stat. Assoc. 46 (253) (1951) 68–78. http://dx.doi.org/10.1080/01621459.1951.10500769.
[36] J.R. Perks, S. Lucero, A.M. Monjazeb, J.J. Li, Anthropomorphic Phantoms for Confirmation of Linear Accelerator-Based Small Animal Irradiation, Cureus URL http://dx.doi.org/10.7759/cureus.254
[37] M.F.W. Festing, 3rs-reduction (2015).URL⟨http://www.3rs-reduction.co.uk⟩